# Study on Morphology, Crystallization Behaviors of Highly Filled Maleated Polyethylene-Layered Silicate Nanocomposites

**Yunchuan Xie,[1,2] Demei Yu,[1,2] Jie Kong,[3] Xiaodong Fan,[3] Wenqiang Qiao[3]**

[1]*State Key Laboratory of Electrical Insulation and Power Equipment, Xi'an Jiaotong University, Xi'an 710049, China*
[2]*Department of Applied Chemistry, School of Science, Xi'an Jiaotong University, Xi'an 710049, China*
[3]*Department of Applied Chemistry, School of Science, Northwestern Polytechnic University, Xi'an 710072, China*

Received 28 April 2005; accepted 15 September 2005
DOI 10.1002/app.23206
Published online in Wiley InterScience (www.interscience.wiley.com).

**ABSTRACT:** The influences of organically modified montmorillonite (MMT) on morphology, crystallization behaviors of maleic anhydride grafted polyethylene (mPE) are investigated by using wide angle X-ray diffraction (WAXD), transmission electron microscopy (TEM), differential scanning calorimetry (DSC), polarized optical microscopy (POM), and dynamic mechanical analysis (DMA). WAXD and TEM results indicate that the molecules of mPE had been inserted into interlayer of the organoclay, and the final morphology of the hybrid changes from exfoliated type to intercalated type gradually with the increasing content of the clay, which is determined by the equilibrium between interfacial interaction of mPE-clay and van der Waals attraction of clay–clay. It is suggested that MMT could affect the crystallization process of mPE in two ways: First, MMT can provide heterogeneous surface and facilitate nucleation step; then, the silicates as diffusion or displacement barriers may restrict the growth step. However, the clay has no significant effects on the total nonisothermal crystallization rate. Otherwise, study on the dynamic mechanical properties show that the storage modulus of the hybrid is around 30% higher than that of the polymer matrix. And the motions of molecular relaxation and conformational transitions both in noncrystalline and crystalline phases are confined by the strong interactions between the polymer and the clay. © 2006 Wiley Periodicals, Inc. J Appl Polym Sci 100: 4004–4011, 2006

**Key words:** morphology; crystallization behaviors; montmorillonite; maleated polyethylene; interfacial interaction

## INTRODUCTION

Polymer-layered silicate nanocomposites have attracted great attention for their academic and industrial importance. There has been an unexpected improvement in their mechanical, thermal, and barrier properties.[1–3] Besides, they can also provide a good model for studying the formation, structure, and phase transitions of organic–inorganic hybrids, which may lead to a better understanding of polymers in a confined environment.[4]

The morphology and crystallization behaviors of polymers can be influenced not only by their own molecular structure, but also by the type and content of foreign fillers, when undergoing heterogeneous nucleating process.[5] It is well known that addition of a rather small quantity filler (<1 wt %) into crystallizable polymers can generally lower their molecular nucleating and folding surface free energy, which may speedup crystallization process, reduce spherulite size, and change the final morphology.[5,6] These additives, which can also be called as nucleating agent, have been successfully utilized in engineering plastics, including PP, PET and PA, and the compounded polymers presented greatly improved mechanical and optical properties.[7,8] However, study of these fillers as nucleating agent on the crystallization behaviors of polyethylene is few. It is because the molecule of polyethylene mainly consists of flexible nonpolar —$CH_2$—$CH_2$— chain segments, and it may crystallize rapidly without regarding so small a quantity of the filler, within the concept of nucleating agents. Nevertheless, if a large amount of filler (>1 wt %) is introduced into polyethylene matrix, the morphology and crystallization behaviors of polymer may be altered. The commonly used silicate filler in recent studies about polymer-layered silicate nanocomposites is montmorillonite (MMT), which is a smectic clay with lamellar crystal structure.[9] To improve the compatibility between the polymer and clay, the clay was usually modified with ion-exchange reaction by various organic cationic surfactants. Besides, another approach was the introduction of polar functional groups, such as maleic anhydride, to the polymer matrix.[10,11]

Until now, the studies are mostly focused on the preparation and mechanical properties of the compos-

*Correspondence to:* Y. Xie (yun_chuanx@hotmail.com).


© 2006 Wiley Periodicals, Inc.

ites. Reports on the influences of interfacial interactions between the grafted polar polymer and organoclay on crystallization behaviors and morphology of the composites are few. In this work, a series of highly filled (~10 wt %) maleated PE/organo-MMT hybrids were prepared by solution blending method. The effect of the interfacial interactions of MMT with the matrix on the morphology and crystallization behaviors of the composites are investigated, and the dynamic mechanical properties of the hybrid under confined environment were also analyzed.

## EXPERIMENTAL

### Materials

Maleic anhydride grafted polyethylene (mPE), which has a weight–average molecular weight of $1.2 \times 10^5$ and a grafting degree of 0.85 wt %, was purchased from Huadou Chemical Co. (Jiangshu Province, China). It was purified before use. At first, mPE was dissolved in boiling xylene and refluxed for 60 min; then, the hot solution was poured into large amount of acetone. The precipitate was collected and dried at 60°C in a vacuum oven for 72 h.[12] Organophilic montmorillonite with a cation exchange capacity value of 100 mequiv./100 g was kindly provided by Chemical Institute of Minerals (Shannxi Province, China), which was ion-exchanged with octadecyl ammonium chloride.

### Nanocomposites preparation

The purified mPE and organo-MMT of various proportions were added into a three-necked flask equipped with a stirrer and a condenser, then xylene was added to form a 1 wt % solution. The temperature was elevated to 120°C and the solution was stirred vigorously for 30 min. After cooling, the solution was filtered and the products were dried at 60°C in a vacuum oven for 72 h. The powdered samples were prepared, and PENC1.5, PENC5, and PENC9 refers to composites containing 1.5, 5, and 9 wt % MMT, respectively.

### Measurements

The differential scanning calorimetry (DSC) measurements were performed on a TA MDSC2910 instrument equipped with refrigerated cooling system. The temperature was always calibrated with indium (156.6°C), and the heat flow rate was calibrated with the heat of fusion of indium (28.71 J/g). The furnace was purged with dry nitrogen at a flow rate of 50 mL/min. (1) *Measurement of degree of crystallinity*: A composite sample of about 5 mg was crimped into an aluminum pan. The sample was heated to 170°C and kept isothermal for 3 min to eliminate the thermal history. Then, the temperature was lowered to 0°C, and the sample was reheated to 170°C to gain the degree of crystallinity ($X_c$). The heating and cooling rates were 10°C/min. The basic equation for calculating $X_c$ of the hybrid via DSC is as follows[13]

$$X_c = \frac{\Delta H}{(1 - \Phi)\Delta H_{100}} \times 100\% \quad (1)$$

where $\Phi$ is the weight percent of MMT; $\Delta H$ is the integrated melting enthalpy; $\Delta H_{100}$ is melting enthalpy of 100% crystalline polyethylene, which is taken as 287.3 J/g in this study.[14,15] $X_c$ was calculated with a software from TA Instrument Co. (2) *Nonisothermal crystallization:* The composite samples of about 5 mg were crimped into aluminum pans. After that, samples were heated to 170°C and kept isothermal for 3 min to eliminate the thermal history. Then, the temperature was lowered to 0°C at cooling rates of 5, 7, 10, 12, and 15°C/min, respectively. The exothermal crystallization peak was recorded as a function of temperature.

A Philips wide-angle X-ray diffractometer, equipped with a graphite homochromatic instrument and a Cu anticathode (40 kV, 35 mA, scanning rate = 1°/min, $2\theta$ = 1.5–10°), was employed to decide the interlayer spacing of MMT. The ambient temperature was 25°C.

The dispersion state of the MMT in the PE matrix was observed by using transmission electron microscopy (TEM) (Hitachi-800, Japan) with an accelerating voltage of 100 kV. A thin layer of about 80 to 100-nm thickness were sectioned from the sample using an ultra-microtome.

The spherulite morphology was observed on the hot stage (Instec-HCS20U, USA) mounted on a polarized optical microscopy (POM) (Nikon-E400POL, Japan), and photographs were taken by a digital camera (Nikon-CoolPix4500, Japan). Samples were hot-pressed into membrane of 0.02 mm thick. After that, the membrane sample was heated to 170°C and kept for 3 min in a hot stage. Then the temperature was lowered to room temperature at a cooling rate of 10°C/min.

Dynamic mechanical measurements were performed on a DMA-Q800 analyzer (TA Instruments, New Castle, DE). Samples were hot-pressed into a membrane of $30 \times 6 \times 1$ mm$^3$ size. After that, experiments were performed in tension mode from −140 to 140°C at a heating rate of 3°C/min. The frequency for the experiments was 5 Hz.

## RESULTS AND DISCUSSION

### Morphologies of mPE/MMT nanocomposites

The morphology of the composites has traditionally been investigated using wide angle X-ray diffraction

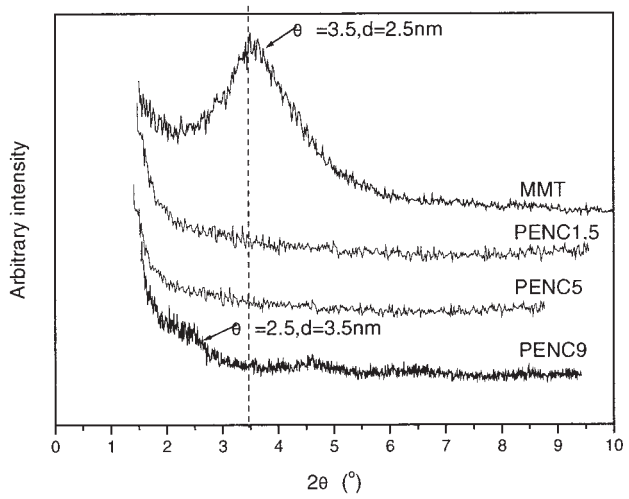


**Figure 1** WAXD patterns for MMT and PENC samples.

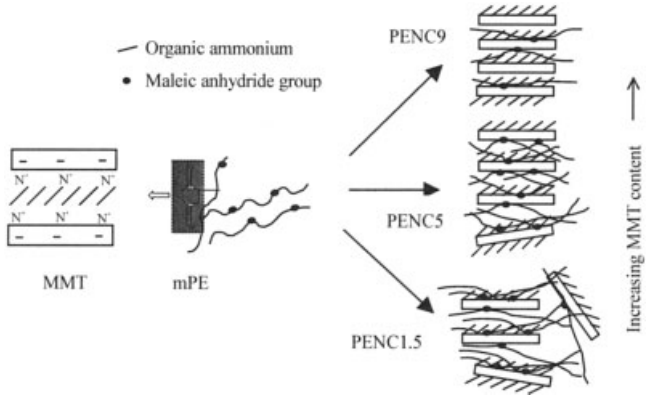


**Figure 3** Structural diagrams for nanocomposites with different MMT content.

(WAXD) and TEM.[16] Figure 1 shows the WAXD patterns of organo-MMT and the composites in low angle range (1.5–10°). As can be seen, organic MMT presents a strong reflection peak at about $2\theta = 3.5°$, which corresponds to an interlayer distance of $d_{001} = 2.5$ nm (calculated by Brag equation: $2d_{001}\sin\theta = \lambda$) for its (001) diffraction face. At the same time, PENC1.5 and PENC5 samples show no obvious reflection peak in the scanning scope. This implies that the mPE molecules had been inserted into the interlayer of the organoclay and greatly enlarged the interlayer distance (>10 nm).[17] PENC9 sample shows a weak reflection peak at about $2\theta = 2.5°$, which corresponds to an interlayer distance of $d_{001} = 3.5$ nm. It also suggests that the interlayer spacing was enlarged to a larger distance by the inserted molecules.[18]

In order to further investigate the dispersion state of the clay in the polymer matrix, TEM study was employed. Figure 2 gives the TEM images for PENC1.5 and PENC5 samples. As can be seen, MMT was dispersed well in PENC1.5 sample. It shows a strip distribution of white field (matrix) alternate with dark lines (silicate layers), which means some silicate layers had been delaminated into the matrix. However, there still exist ordered silicate conglomerations in the image, and the dimension of these conglomerations is too small to present a reflection peak in WAXD patterns. This is a typical morphology of partially delaminated nanocomposite. TEM photograph for PENC5 sample presents large-sized silicate conglomerations, and some molecules had also been inserted into layers of the clay. This is a typical morphology of partially unordered intercalated nanocomposite.[19] These results are in accordance with the WXRD data shown in Figure 1.

Figure 3 shows a schematic representation of the intercalation process of the clay into mPE matrix. According to the thermodynamic theory ($\Delta G = \Delta H - T\Delta S$), if the entropic penalty for confinement of polymer chains is overcome by the enthalpic gain from polymer–clay interactions ($\Delta G < 0$), the intercalation occurs through the penetration of mPE molecules into the interlayer spaces of the silicates. When the interlayer spacing becomes large enough by the

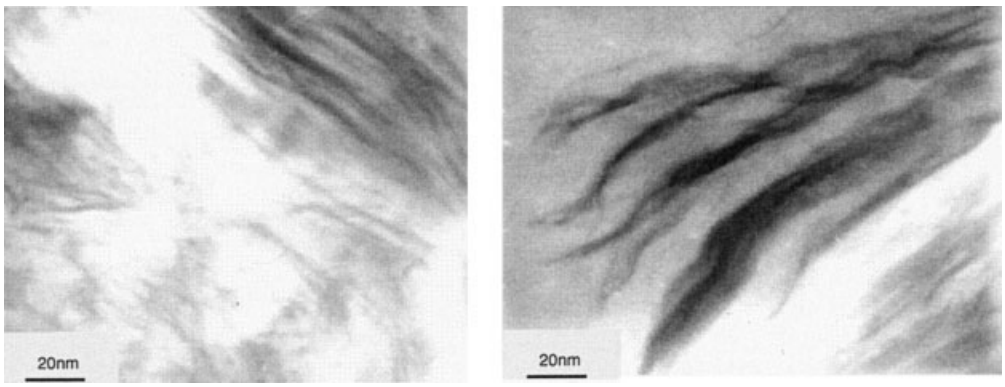


**Figure 2** TEM images for PENC1.5 (left) and PENC5 (right) samples.

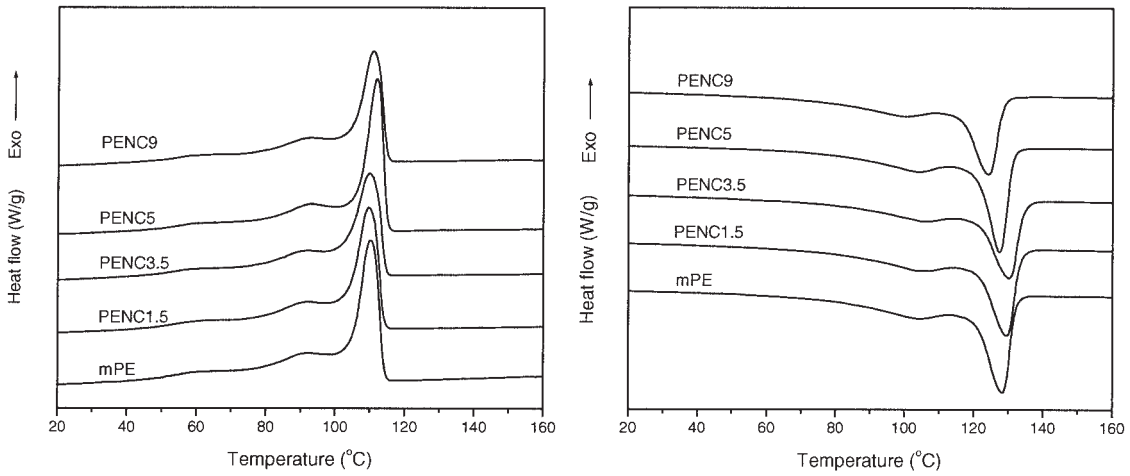


**Figure 4** DSC crystallization and melting curves for mPE and PENC samples.

extensive penetration of mPE molecules to overcome the van der Waals interaction between the adjacent silicate layers, exfoliation occurs to form nano-dispersed silicates in the matrix.[19,20] In this study, the driving force for formation of intercalated structure is mainly attributed to the electrostatic interaction between the ammonium ions and the electrical charges on the polar maleic anhydride groups. When the clay content is low, for example 1.5 wt %, the interfacial interaction between mPE molecules and clay is strong enough to overcome the attraction of well-dispersed silicate layers and partially delaminated morphology formed; however, when the clay content is high, for example 5 wt %, agglomerated-silicate occurred and van der Waals force between adjacent layers is strong, thus intercalated morphology formed. So, there may present various morphologies with different content of clay as shown in Figure 3.

### Crystallization behaviors of mPE/MMT nanocomposites

Figure 4 presents the crystallization and melting DSC curves for pure mPE and PENCs, respectively. Table I lists characteristic values of these curves. As can be seen, the filler has no significant influence on the crystallization and melting process of sample PENC1.5 and PENC3.5. Compared with the pure matrix, the onset temperature of crystallization ($T_c$), peak temperature of crystallization ($T_p$), and the degree of crysallinity ($X_c$) keep nearly constant. This is different from that of PP and PA.[21,22] While for PENC5, not only the $T_c$ and $T_p$ shifted to higher temperature, but also the $X_c$ was increased by 4%. It is suggested that there exist two competing aspects during the crystallization process of the composites. First, the clay can provide heterogeneous surface and increase the nucleating rate of macromolecules; then, the interfacial interactions between surface of organoclay and polar maleic anhydride groups of grafted chains impeded the motions of molecules and lowered the growing rate.[23–25] Obviously, the content of clay determined the relative dominating status of the two aspects, which also determined the crystallization behaviors of the composites. For PENC1.5 and PENC3.5 samples, the clay may be well dispersed and the effects of the two aspects is countervailed; while for PENC5, ag-

**TABLE I**
**Parameters of Crystallization and Melting Process for mPE and PENC Samples**

| Samples | $T_c^a$ (°C) | $T_p^b$ (°C) | $\Delta H_c^c$ (J/g) | $T_m$ (°C) | $\Delta H_m^d$ (J/g) | $X_c^e$ (%) |
|---|---|---|---|---|---|---|
| mPE | 114.5 | 110.2 | 160.6 | 128.2 | 145.6 | 50.7 |
| PENC1.5 | 114.8 | 109.5 | 162.7 | 129.5 | 145.5 | 50.7 |
| PENC3.5 | 115.1 | 110.0 | 152.9 | 130.2 | 139.1 | 49.8 |
| PENC5 | 116.0 | 112.0 | 164.8 | 127.4 | 150.0 | 54.5 |
| PENC9 | 115.7 | 111.3 | 142.6 | 124.2 | 122.9 | 47.3 |

[a] Onset crystallization temperature.
[b] Crystallization peak temperature.
[c] Crsta1lization enthalpy (150–20°C).
[d] Melting enthalpy.
[e] Apparent crystallinity (20–150°C).

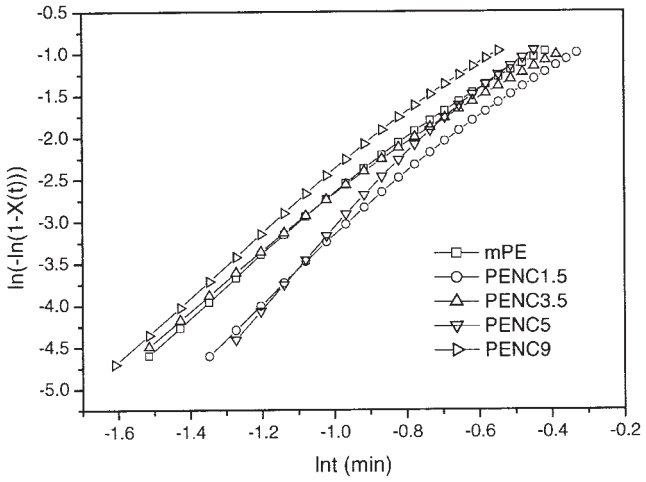


**Figure 5** Nonisothermal crystallization process of mPE and PENC samples by Jeziorny Equation at a cooling rate of 10°C/min.

glomerated clay occurred and the former aspect seems to be dominated. As for PENC9, it seems that the latter aspect becomes dominated, which increases the amount of defects in crystals and lowers the crystallinity.[21]

It can also be seen from Table I that the melting points ($T_m$) of PENCs vary with different content of clay. As for PENC1.5 and PENC3.5, the clay can be well dispersed in the matrix and is helpful to form much thicker lamellar, which improved the melting points. While for PENC5 and PENC9, agglomerated MMT may cause defects and lower the melting points.

### Nonisothermal crystallization behaviors of mPE/MMT nanocomposites

The Jeziorny equation, the modified Avrami equation, is used to describe nonisothermal crystallization kinetics of mPE and the nanocomposites

$$1 - X(t) = \exp(-Zt^n) \tag{2}$$

where the exponent $n$ is a mechanism constant that depends on the type of nucleation and growth process, and $Z$ is an overall constant of the crystallization process involving both nucleation and growth rate parameters. By using the above equation in the double-logarithmic form

$$\ln(-\ln(1 - X(t))) = \ln Z + n\ln t \tag{3}$$

and plotting ln(-ln(1-$X(t)$)) against ln$t$ for each cooling rate, a straight line is obtained with the data at a low degree of crystallinity (<30%) as shown in Figure 5.[26] Thus, $Z$ and $n$ can be estimated through linear fitting. Considering the cooling rate, Jeziorny modified $Z$ by the following equation[27]

$$\lg Z_c = \frac{\lg Z}{\Phi} \tag{4}$$

where $\Phi$ is the cooling rate. The related parameters are listed in Table II.

From Table II it can be seen that for a certain cooling rate, there is no significant difference in the values of $n$, and only when the clay loading exceeded 5 wt % did the $Z_c$ increase and $t_{1/2}$ decrease slightly. This trend is consistent with the results of Figure 4 and Table I, as had been discussed in the preceding section. Since polyethylene is a rapidly crystallized polymer, high clay content (~5 wt %) may increase the rate of crystallization, due to the increase in nucleation sites; while at much higher concentrations, the rate was lowered because of the barrier effect. When the clay loading is very low (~1 wt %), the possible reason for the unobvious nucleating effect maybe that the partial miscibility between mPE molecules and the organic modifiers on the clay surface hindered the crystallization. Therefore, although the clay can facilitate the nucleating process, it has little effects on the total nonisothermal crystallization rate of the composites.

**TABLE II**
**Nonisothermal Crystallization Kinetics Parameters for mPE and PENC Samples**

| | Φ (°C/min) | | | | |
|---|---|---|---|---|---|
| Sample | 5 | 7 | 10 | 12 | 15 |
| mPE | | | | | |
| $n$ | 3.71 | 3.47 | 3.29 | 3.43 | 3.20 |
| $Z_c$ | 0.79 | 0.95 | 1.12 | 1.20 | 1.30 |
| $t_{1/2}$ (min) | 1.25 | 0.97 | 0.75 | 0.68 | 0.60 |
| PENC1.5 | | | | | |
| $n$ | 4.16 | 4.06 | 3.46 | 3.45 | 3.20 |
| $Z_c$ | 0.79 | 0.91 | 1.04 | 1.08 | 1.14 |
| $t_{1/2}$ (min) | 1.33 | 1.08 | 0.83 | 0.77 | 0.67 |
| PENC3.5 | | | | | |
| $n$ | 4.01 | 3.71 | 3.05 | 3.09 | 3.06 |
| $Z_c$ | 0.86 | 0.95 | 1.03 | 1.06 | 1.08 |
| $t_{1/2}$ (min) | 1.32 | 1.03 | 0.80 | 0.73 | 0.68 |
| PENC5 | | | | | |
| $n$ | 4.43 | 4.25 | 4.18 | 3.84 | 3.32 |
| $Z_c$ | 0.92 | 1.01 | 1.19 | 1.23 | 1.36 |
| $t_{1/2}$ (min) | 1.13 | 0.88 | 0.71 | 0.62 | 0.52 |
| PENC9 | | | | | |
| $n$ | 3.72 | 3.61 | 3.52 | 3.34 | 3.12 |
| $Z_c$ | 0.93 | 0.98 | 1.03 | 1.09 | 1.12 |
| $t_{1/2}$ (min) | 1.03 | 0.82 | 0.67 | 0.57 | 0.45 |

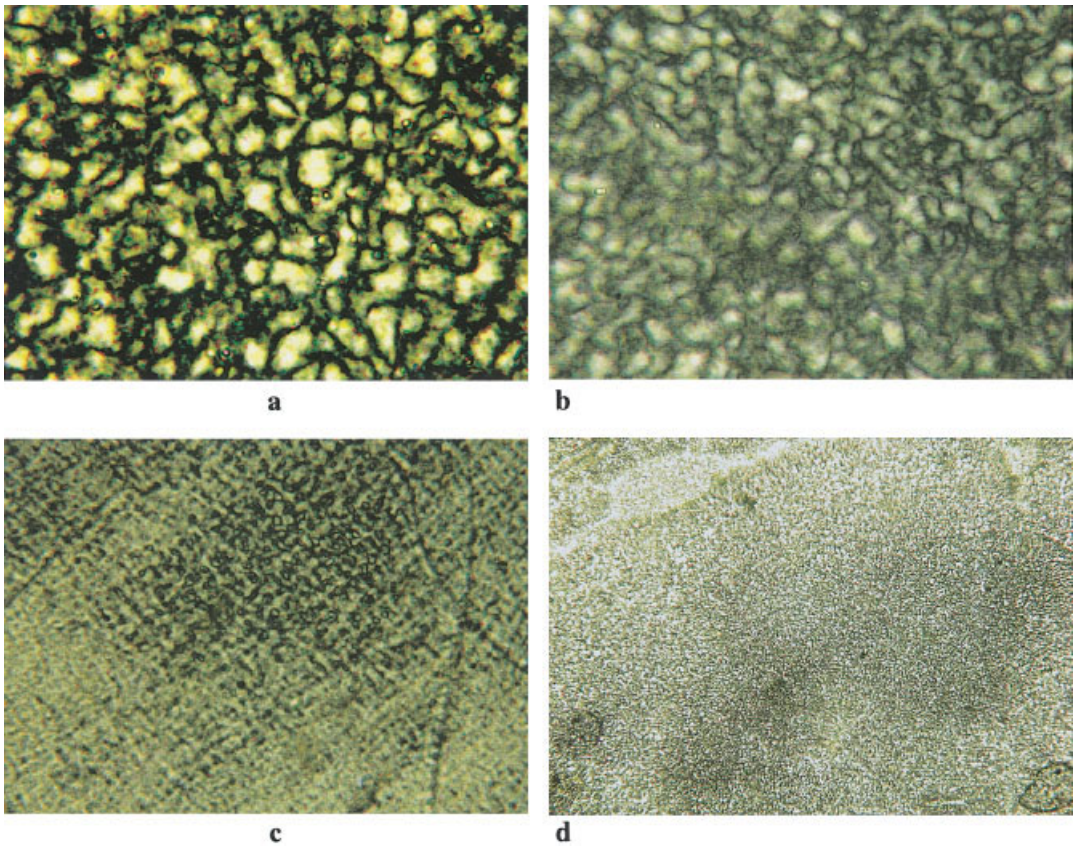


**Figure 6** POM photos for (a) mPE, (b) PENC1.5, (c) PENC5, and (d) PENC9 (×200). [Color figure can be viewed in the online issue, which is available at www.interscience.wiley.com.]

### Anisotropic phase structure of mPE/MMT nanocomposites

Figure 6 shows the typical spherulitic texture for pure matrix (mPE) and the nanocomposites (PENCs). Apparently, the spherulite size gradually decreases with the increasing content of MMT.

This phenomenon is attributed to the nucleation effect of dispersed clay, which provide much more heterogeneous nuclei and reduce the size of spherulite. At the same time, both the strong interactions of polymer with clay and barrier effect of clay constrained the diffusing motions and conformational transitions of molecules during crystal growing step, which caused more defects in crystals and diminished the spherulite size.[28,29]

### Dynamic mechanical properties of mPE/MMT nanocomposites

Figure 7 presents the dynamic mechanical properties of mPE and PENCs, respectively. Table III lists the peak temperature of related relaxations. From storage modulus-temperature curves, it can be seen that the dynamic modulus of PENCs is 20–30% higher than that of pure matrix during the low temperature region (<0°C). And the order is: PENC5 > PENC1.5 > PENC9 > mPE. The increased modulus not only contributed to the fine dispersion of silicate clay but also to the physical crosslinking effect induced by the strong interactions between the polymer and the clay. However, excessive clay may produce serious conglomerations and restrict the crystallization, so as to lower the mechanical modulus.

The $\beta$ transition of the hybrid is related to the motions of branching chains, and the relative activity of molecules may be characterized by the intensity of its transiting peak. Suppose, the intensity of $\beta$ transition for mPE is 1, the relative intensity of $\beta$ transitions for PENC1.5, PENC5, and PENC9 are 0.96, 0.89, and 0.65, respectively. Evidently, the activity of branching chains was intensively weakened by the interfacial interaction between polar groups-grafted molecules and surface of organically modified clay. The $\gamma$ transition generally corresponds to the crank motion of three to five $CH_2$ chain segments. Compared with pure mPE, the peak temperatures for PENCs were increased by 2–3°C. This may also be explained to that of the electrostatic interactions between the polymer and the clay restricted the mobility of related chain segments. As can been seen from Figure 7, the peak

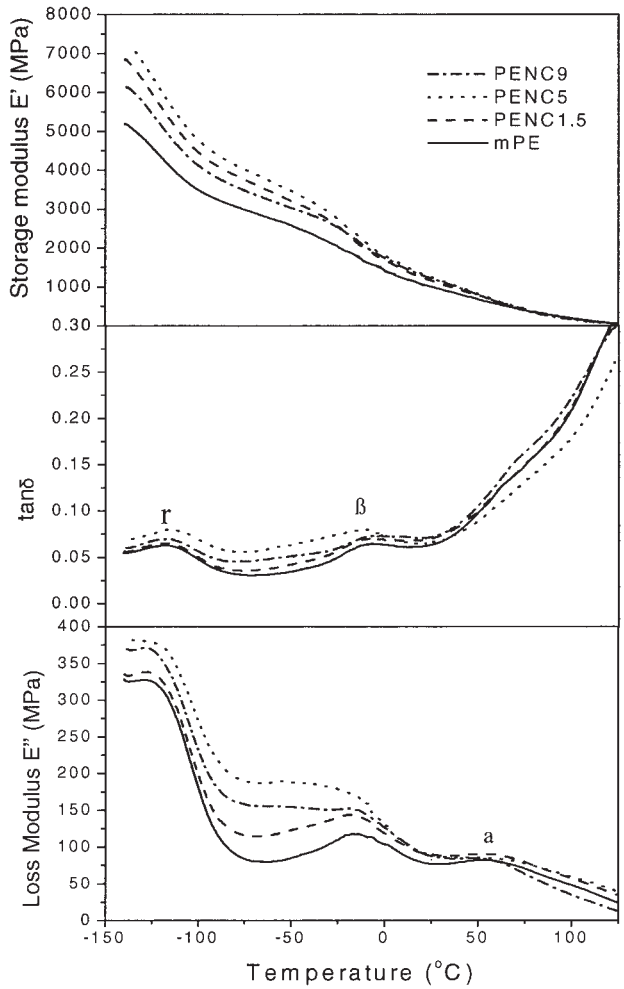


**Figure 7** DMA curves for mPE and PENC samples.

position of $\alpha$ transition for PENCs moves to higher temperature. This suggests that the dispersed clay can not only limit the molecular motion in amorphous region but also confine the segmental relaxation in crystalline region.

In a word, the molecules of maleated polyethylene can be inserted into layers of organo-MMT via the strong interfacial interactions between the polymer and the clay, and the crystallization behaviors of the polymer matrix may be restricted by the interactions and barrier effect of MMT. This may change the final morphology and macromolecular relaxations of the hybrid.

**TABLE III**
**DMA Peak Temperature of Transitions within mPE and PENC Samples**

| Sample | $\alpha$ (°C) | $\beta$ (°C) | $\gamma$ (°C) |
|---|---|---|---|
| mPE | 57 | −17 | −116 |
| PENC1.5 | 58 | −18 | −114 |
| PENC5 | 61 | −16 | −113 |
| PENC9 | 58 | −16 | −114 |

## CONCLUSIONS

The results of WAXD and TEM indicate that the morphology of maleated PE/organo-MMT nanocomposites changes from exfoliated type to intercalated type gradually with the increasing content of MMT, which is decided by the equilibrium between interfacial interactions of mPE-clay and van der Waals attraction of clay-clay.

The chemical bonding between the maleic anhydride groups of PE molecules and organic ammonium greatly improved the compatibility of the polymer and clay. As a result, the crystallization behaviors of the polymer matrix can be affected in two ways. First, the clay can provide heterogeneous nuclei during nucleation step; then, it may restrict the conformational transitions of molecules during growth step. Although, the clay can reduce the size of spherulite, it has no significant effect on the total nonisothermal crystallization rate.

The peak positions for $\alpha$ transition and $\gamma$ transition of the composites shift to higher temperature, while the intensity for $\beta$ transitions decreases. This suggests that the molecular motions and conformational transitions both in noncrystalline and crystalline phases are significantly confined by the strong interactions between the polymer and the clay.

## References

1. Kurokawa, Y.; Yasuda, H.; Kashiwagi, M.; Oyo, A. J Mater Sci Lett 1997, 16, 1670.
2. Lepoittevin, B.; Pantoustier, N.; Devalckenaere, M.; Alexandre, M.; Kubies, D.; Calberg, C.; Jerome, R.; Dubois, P. Macromolecules 2002, 35, 8385.
3. Xu, R. J.; Manias, E.; Synder, A. J.; Runt, J. Macromolecules 2001, 34, 334.
4. Giannelis, E. P.; Krishnamoorti, R.; Manias, E. Adv Polym Sci 1999, 138, 107.
5. Kristiansen, M.; Werner, M.; Tervoort, T.; Smith, P.; Blomenhofer, M.; Schmidt, H.-W. Macromolecules 2003, 36, 5150.
6. Feng, Y.; Jin, X.; Hay, J. N. J Appl Polym Sci 1998, 69, 2089.
7. Chen, Y.; Xu, M.; Li, Y. Y.; He, J. S. Chin Acta Polym Silica 1999, 1, 7.
8. Mudru, I.; Balazs, G. J Therm Anal 1998, 52, 355.
9. Ray, S.; Okamoto, M. Prog Polym Sci 2003, 28, 1539.
10. Zhao, Z.; Tang, T.; Qin, Y.; Huang, B. Langmuir 2003, 19, 7157.
11. Koo, C. M.; Han, H. T.; Kim, S. O.; Wang, K. H.; Chung, I. J. Macromolecules 2002, 35, 5116.
12. Yin, J.; Zhang, J. Chin J Funct Polym 2002, 15, 99.
13. Blundell, D. J.; Beckett, D. R.; Willcocks, P. H. Polymer 1981, 22, 704.
14. Wunderlich, B.; Cormier, C. M. J Polym Sci Part A: Polym Chem 1967, 5, 987.
15. Mirabella, F. M.; Bafna, A. J Polym Sci Part B: Polym Phys 2002, 40, 1637.
16. Liu, Z. J.; Chen, K. Q.; Yan, D. Y. Eur Polym J 2003, 39, 2359.
17. Alexandre, M.; Dubois, P.; Sun, T. Polymer 2002, 43, 2123.

18. Ma, J. S.; Qi, Z. N.; Zhang, S. F. Chem J Chinese Univ 2001, 22, 1767.
19. Qi, Z. N.; Shang, W. Y. Theory and Practice of Polymer/Silicate Nanocomposites; Chinese Chemical Industry Press: China, 2002.
20. Koo, C. M.; Kim, S. O.; Chung, I. J. Macromolecules 2003, 36, 2748.
21. Ma, J. S.; Zhang, S. M.; Qi, Z. N.; Li, G.; Hu, Y. L. J Appl Polym Sci 2002, 83, 1978.
22. Wu, Z. G.; Zhou, C. X.; Zhu, N. Polym Test 2002, 21, 479.
23. Xu, W. B.; Ge, M. L.; He, P. S. Chin Acta Polym Silica 2001, 5, 584.
24. Ma, J. S.; Zhang, S. M.; Qi, Z. N. Chem J Chinese Univ 2002, 23, 734.
25. Gu, Q.; Wu, D. C.; Yi, G. Z. Chem J Chinese Univ 1999, 20, 324.
26. Liang, G.; Xu, J.; Xu, W. J Appl Polym Sci 2004, 91, 3054.
27. Jeziorny, A. Polymer 1978, 19, 1142.
28. Jiang, S. Ch.; Ji, X. L.; An, L. J.; Jiang, B. Zh. Polymer 2001, 42, 3901.
29. Zhang, Q.; Peng, M.; Yi, X. S. Mater Lett 1999, 40, 91.